

Glutamatergic Signaling Maintains the Epithelial Phenotype of Proximal Tubular Cells

Milica Bozic,* Johan de Rooij,[†] Eva Parisi,* Marta Ruiz Ortega,[‡] Elvira Fernandez,* and José M. Valdivielso*

*Nephrology Research Department, IRB Lleida, University Hospital Arnau de Vilanova, Lleida, Spain; [†]Hubrecht Institute and University Medical Centre Utrecht, Utrecht, The Netherlands; and [‡]Laboratory of Nephrology, Foundation Jimenez Diaz, Madrid, Spain

ABSTRACT

Epithelial–mesenchymal transition (EMT) contributes to the progression of renal tubulointerstitial fibrosis. The *N*-methyl-D-aspartate receptor (NMDAR), which is present in proximal tubular epithelium, is a glutamate receptor that acts as a calcium channel. Activation of NMDAR induces actin rearrangement in cells of the central nervous system, but whether it helps maintain the epithelial phenotype of the proximal tubule is unknown. Here, knockdown of NMDAR1 in a proximal tubule cell line (HK-2) induced changes in cell morphology, reduced E-cadherin expression, and increased α -SMA expression. Induction of EMT with TGF- β 1 led to downregulation of both E-cadherin and membrane-associated β -catenin, reorganization of F-actin, expression of mesenchymal markers *de novo*, upregulation of Snail1, and increased cell migration; co-treatment with NMDA attenuated all of these changes. Furthermore, NMDA reduced TGF- β 1–induced phosphorylation of Erk1/2 and Akt and the activation of Ras, suggesting that NMDA antagonizes TGF- β 1–induced EMT by inhibiting the Ras-MEK pathway. In the unilateral ureteral obstruction model, treatment with NMDA blunted obstruction-induced upregulation of α -SMA, FSP1, and collagen I and downregulation of E-cadherin. Taken together, these results suggest that NMDAR plays a critical role in preserving the normal epithelial phenotype and modulating tubular EMT.

J Am Soc Nephrol 22: 1099–1111, 2011. doi: 10.1681/ASN.2010070701

Epithelial–mesenchymal transition (EMT) represents a dynamic course of events that characterizes physiologic developmental processes and pathologic conditions such as fibrosis and carcinogenesis.^{1,2} Tubular EMT has been described as one of the key mechanisms in the pathogenesis of renal fibrosis,³ where fibroblast activation represents an important pathway for progression of chronic kidney disease.⁴ *In vivo* and *in vitro* studies indicate that the major percentage of fibroblasts in the damaged kidney could originate from the tubular epithelium through the process of EMT.^{5,6} In the unilateral ureteral obstruction (UUO) model of kidney fibrosis, Iwano *et al.*⁵ showed that 36% of interstitial fibroblasts originate from EMT of tubular epithelial cells. Tubular EMT is characterized by the loss of intercellular contacts caused by the downregulation of E-cadherin, relocation of β -catenin from the cell periphery into the nucleus, *de novo* expression of

α -SMA and vimentin, actin cytoskeleton reorganization, tubular basement membrane destruction, and enhanced cell migration.^{2,7}

The *N*-methyl-D-aspartate receptor (NMDAR) is a member of a heterogeneous family of ionotropic glutamate receptors, with important roles within the CNS.⁸ NMDAR is a heteromeric protein composed of an essential NR1 subunit combined with

Received July 5, 2010. Accepted February 9, 2011.

Published online ahead of print. Publication date available at www.jasn.org.

E.F. and J.M.V. share senior authorship.

Correspondence: Dr. José Manuel Valdivielso, Nephrology Research Laboratory, IRB LLEIDA, University Hospital Arnau de Vilanova, Rovira Roure 80, 1^a Planta, 25198 Lleida, Spain. Phone: 349-7300-3650; Fax: 349-7370-2213; E-mail: valdivielso@medicina.udl.cat

Copyright © 2011 by the American Society of Nephrology

one or more NR2 subunits⁹ that form a channel highly permeable to Ca^{2+} . Activation of NMDAR requires simultaneous binding of glutamate and glycine, leading to the channel opening and Ca^{2+} influx. NMDA, a non-metabolic agonist of NMDAR, mimics the action of glutamate regulating only this receptor. In addition to NMDAR's broad distribution in neurons, it has become evident that functional NMDAR is also expressed in a variety of non-neuronal cells and tissues.^{10–16} Importance of NMDAR in the kidney and its functional role has emerged as an interesting research topic, although experimental data are scarce. Results from Deng *et al.*¹⁶ showed the presence of NMDAR1 subunit in the basolateral proximal tubules of the rat kidney and confirmed a role for renal NMDAR in the regulation of renal vasodilatation. Recently, this group showed that renal NMDARs independently stimulate proximal tubular reabsorption and glomerular filtration.¹⁷ Furthermore, it has recently been reported that NMDAR is present in podocytes where glutamatergic signaling contributes to the integrity of the glomerular filtration barrier.¹⁸ However, the function of NMDAR in tubular cells is not yet fully understood.

A wide spectrum of cellular functions in a variety of cell types is being controlled by the activity of ion channels. Although the activity of calcium channels is important in the regulation of cell migration,^{19–22} calcium signaling is significant in mediating actin rearrangement^{23,24} and organization of cadherins and catenins into intercellular junctions.²⁵ Indeed, NMDAR activation has been shown to induce changes in actin organization in cerebellar granule cells²⁶ and retinal neurons²⁷ and to inhibit cell migration in neurons¹⁹ and keratinocytes.²⁰ Taking into consideration knowledge of multiple characteristics of NMDAR in a variety of tissues, including renal itself, we sought to examine its role in the maintenance of the epithelial phenotype of proximal tubular epithelial cells (PTECs) and in tubular EMT *in vitro*. Furthermore, we examined the role of channel activation in tubulointerstitial fibrosis induced by UUO in mice.

RESULTS

NMDAR Subunit mRNA Expression in Human PTECs

Figure 1 shows the relative expression of NMDAR subunits in HK-2 cells (human renal proximal tubular epithelial cells immortalized by transduction with human papilloma virus 16 E6/E7 genes). The results show that both NMDAR1 and NMDAR2B are expressed in this cell line. Thus, a functional NMDAR is expected to be present in HK-2.

NMDA Treatment Increases the Ca^{2+} Influx into the HK-2 Cell

To examine whether NMDAR activation in HK-2 led to an influx of Ca^{2+} through the channel, cells were loaded with

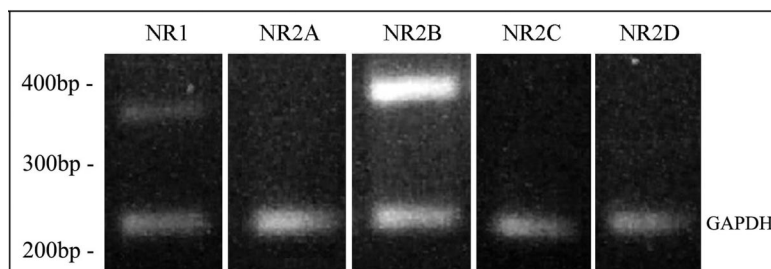


Figure 1. HK-2 cells express both NR1 and NR2B subunit of NMDAR. Total RNA was submitted to RT with an oligo dT reverse primer followed by PCR with different set of primers for NMDAR subunits and GAPDH as an internal control. Representative image after agarose gel electrophoresis shows differential expression of investigated receptor subunits (NMDAR1~370 bp; NR2A~300 bp; NR2B~376 bp; NR2C~397 bp; NR2D~280 bp).

Fluo-4 and incubated with NMDA. The treatment induced significant influx of Ca^{2+} into the cell, seen as a time-dependent elevation in fluorescence signal detected by the calcium-sensitive fluorophore (Supplementary Video 1).

Knockdown of NMDAR1 Influences PTEC Phenotype

To assess the function of the channel in basal conditions, the expression of the NMDAR1 subunit was disrupted by short hairpin RNA (shRNA). Figure 2, A and B, shows an evident decrease in NMDAR1 expression in HK-2 infected with FSVsi-NMDAR1 (shNR1) compared with FSVsi (control). Strikingly, downregulation of NMDAR1 in HK-2 induced changes in the epithelial phenotype, evident as a decrease of E-cadherin (Figure 2, C and D) and an increase of alpha-smooth muscle actin (α -SMA) (Figure 2, E and F), with the changes in cell morphology toward the loss of cobble-stoned shape and the acquisition of spindle-like form of loosely interconnected cells (Figure 2, G and H). These results point to a role of basal activation of NMDAR in maintaining the epithelial phenotype.

NMDAR Activation Reduces TGF- β 1-Induced EMT *In Vitro*

Once it was determined that basal NMDAR activation had a role in preserving the epithelial phenotype, we sought to assess whether activation of the channel could be a possible strategy in decreasing the change of phenotype in TGF- β 1-induced EMT. Compared with control, TGF- β 1-treated cells started to lose epithelial E-cadherin and gained α -SMA (Figure 3, A and B), whereas co-treatment with NMDA restored expression of these molecules to the control level (Figure 3, A and B). Co-incubation with TGF- β 1 and Thapsigargin (TG) did not result in restoration of E-cadherin and α -SMA expression in HK-2 (Figure 4, A and B), suggesting a specific effect of Ca^{2+} entry through NMDAR. Treatment with TGF- β 1 caused upregulation of Snail1 in HK-2 within 6 hours (Figure 3, C and D) and phosphorylation of Smad2/3 and its translocation into the nucleus within 120 minutes after stimulation (Figure 3, E and F), which was blunted by co-treatment with NMDA. Co-incubation with an antagonist of NMDAR (MK-801) abolished the inhibitory effect of NMDA on TGF- β 1-induced upregulation

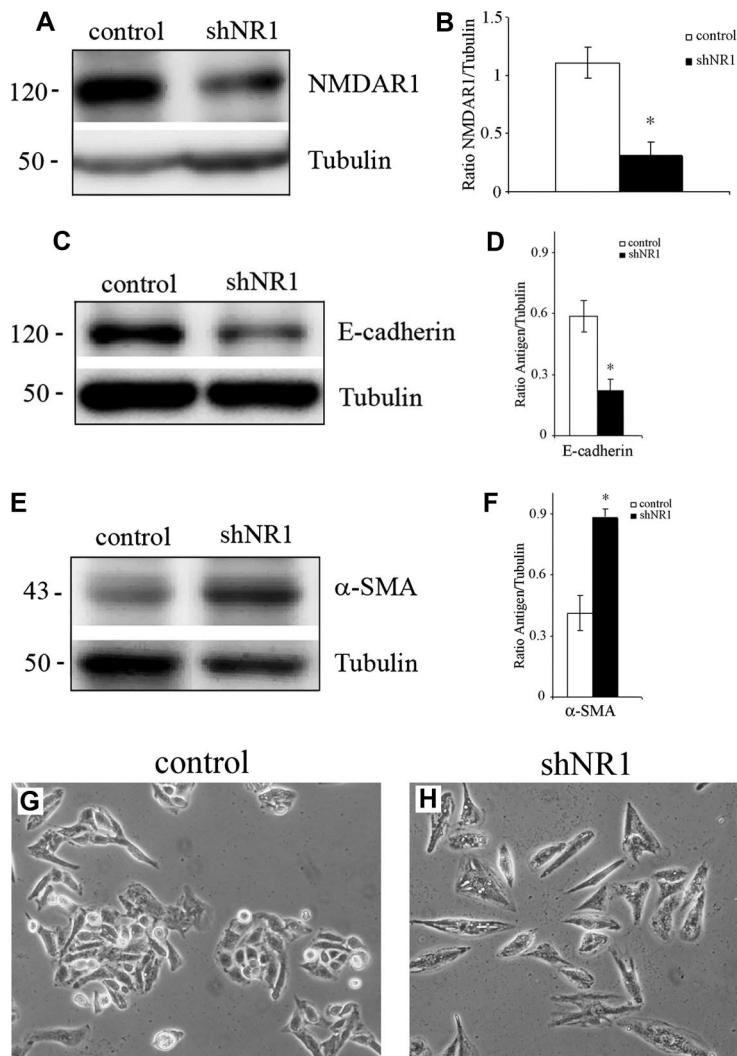


Figure 2. NMDAR1 gene knockdown originates loss of epithelial phenotype in PTECs. Representative Western blot (A) and quantitative analysis (B) show a decrease in NMDAR1 expression in HK-2 infected with FSVsi-NMDAR1 (shNR1) compared with FSVsi (control); $*P < 0.05$ versus control. Downregulation of NMDAR1 in HK-2 induced changes in epithelial phenotype, evident as a decrease of E-cadherin (C and D) and an increase of α -SMA (E and F). $*P < 0.05$ versus control. (G and H) Representative photomicrographs show morphologic changes in the shNR1 group of cells (H) compared with control (G). Magnification: $\times 20$.

of Snail1, showing that the effect of NMDA was achieved through the activation of the channel (Figure 4G). To confirm that the influx of Ca^{2+} through the activated NMDAR is the one responsible for the preservation of the epithelial phenotype, we performed experiments in Ca^{2+} -free medium. In the absence of Ca^{2+} in the medium, NMDAR activation failed to ameliorate TGF- β 1-induced downregulation of E-cadherin and upregulation of Snail1 in HK-2 (Figure 4, H and I), as well as to preserve characteristic cobble-stoned morphology of tubular cells (Figure 4L), pointing again to an increase in extracellular Ca^{2+} flux as the responsible for NMDA effect.

TGF- β 1 induced significant changes in F-actin organization seen as a strong increase in Phalloidin fluorescence,

whereas co-treatment with NMDA inhibited these changes (Figure 5A). NMDA alone for 24 hours induced a significant decrease of cellular F-actin in HK-2 (Figure 5A). To rule out the possibility that changes in F-actin distribution were caused by changes in cell volume, cell size was measured. NMDA did not induce changes in cell volume (Supplementary Figure 1C).

TGF- β 1 induced a loss of cobble-stoned morphology and acquisition of spindle-like shape, whereas co-treatment with NMDA restored the epithelial phenotype of HK-2 (Figure 5C). Immunofluorescence showed strong upregulation of vimentin in TGF- β 1-treated cells (72 hours; Figure 5B) and translocation of β -catenin into the nucleus (24 hours; Figure 5D), whereas co-treatment with NMDA decreased expression of vimentin and restored β -catenin to its original localization (Figure 5, B and D, respectively).

NMDAR Activation Alters Human PTEC Migration *In Vitro*

Wound Healing and Transwell Migration Assay.

The role of NMDAR in human PTEC migration was studied using two different migration assays. In the wound migration assay, NMDA treatment reduced basal (Figure 6, G, H, and J; 48 hours) and TGF- β 1-stimulated cell migration (Figure 6, A–F, J; 48 hours) after 24 and 48 hours. The transwell migration assay followed the same pattern. As shown in Figure 6, I and K, NMDA reduced basal and TGF- β 1-stimulated cell migration after 24 hours. To ensure that the decrease in migration was not caused by the reduced cell viability, an MTT (3-[4,5-dimethylthiazol-2-yl]-2,5-diphenyltetrazolium bromide) assay was performed. NMDA did not modify cell viability (Supplementary Figure 1A).

Time-Lapse Phase Contrast Microscopy.

During migration, cells use different migrational modes to move with varying degrees of speed and directionality²⁸; therefore, we examined the effect of NMDA on cell velocity and persistence using time-lapse phase contrast microscopy. After 24 hours, NMDA reduced basal level of cell persistence on fibronectin, as well as TGF- β 1-induced increase in cell persistence on both tested matrices (Supplementary Figure 2A).

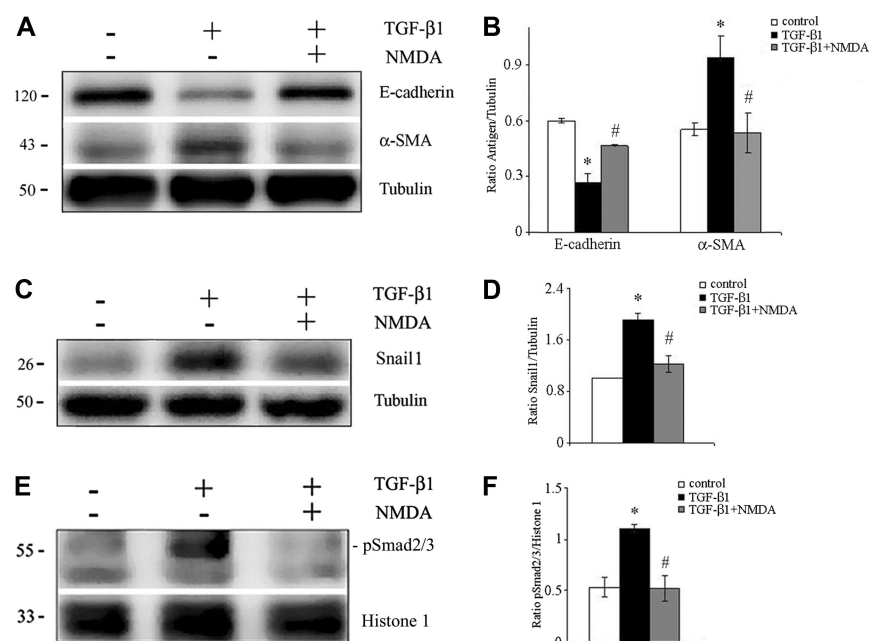


Figure 3. NMDAR activation restored expression of E-cadherin, α -SMA, Snail1, and pSmad2/3 altered by TGF- β 1. HK-2 cells were incubated in serum-free medium (control), TGF- β 1, or TGF- β 1 + NMDA for 72 hours (E-cadherin, α -SMA), 6 hours (Snail1), or 120 minutes (pSmad2/3). Whole cell lysates were immunoblotted with antibodies against E-cadherin, α -SMA, and Snail1. The same samples were reprobed with tubulin to ensure equal loading. Representative Western blots and quantitative analysis show a decrease in E-cadherin (A and B) and an increase in α -SMA (A and B) and Snail 1 (C and D) expression induced by TGF- β 1. Co-treatment with NMDA restored expression of these molecules close to control levels. (E and F) NMDA managed to reduce TGF- β 1-induced translocation of pSmad2/3 into the nucleus after 120 minutes (nuclear extracts). Histone 1 was used as a loading control for pSmad2/3 expression. (B, D, and F) * $P < 0.05$ versus control; # $P < 0.05$ versus TGF- β 1.

To get more insights into the nature of PTEC migration, we analyzed cell velocity. NMDA caused statistically significant reduction of basal and TGF- β 1-induced cell velocity on both tested matrices (Supplementary Figure 2B).

NMDAR Activation Reduces Phosphorylation of Erk1/2 and Akt and Blocks Activation of Ras Induced by TGF- β 1

Treatment of HK-2 with TGF- β 1 resulted in a rapid increase in phosphorylation of Akt (Figure 7, A and B) and Erk1/2 (Figure 7, C and D) within 60 and 30 minutes after stimulation, respectively, which was reduced by co-treatment with NMDA. As shown in Figure 7, E and F, TGF- β 1 caused rapid activation of Ras within 10 minutes after stimulation, whereas co-treatment with NMDA managed to reduce Ras-GTP down to control levels. Co-incubation with TGF- β 1 and TG did not have the same effect on activation of Ras (Figure 4, E and F) and phosphorylation of Erk1/2 (Figure 4, C and D) as NMDA treatment, pointing to specific effects of Ca^{2+} entry through NMDAR. Furthermore, in the absence of Ca^{2+} in the medium, NMDAR activation failed to reduce phosphorylation of Erk1/2 and Akt (Figure 4, J and K), suggesting again that the effect of NMDA is mediated through increasing Ca^{2+} influx.

NMDA Preserves Epithelial Phenotype and Attenuates Renal Fibrosis In Vivo

To study whether the effects of NMDA *in vitro* could have a role in an *in vivo* model of EMT, mice underwent UO and were treated with NMDA. UO induced marked upregulation of α -SMA and type 1 collagen at 5 (Figure 8A) and 15 days (Figure 8B) after surgery compared with contralateral controls. Administration of NMDA significantly decreased α -SMA mRNA expression in obstructed kidneys at both time points (Figure 8, A and B). NMDA treatment showed a tendency to reduce collagen I mRNA 5 days after UO (Figure 8A), whereas at day 15 after UO, NMDA managed to significantly diminish expression of collagen I in obstructed kidneys (Figure 8B). Figure 8, D–F, shows a significant increase of α -SMA protein in the obstructed kidneys at days 5 and 15 after UO compared with contralateral controls. In accordance with mRNA data, NMDA treatment inhibited α -SMA at the protein level (Figure 8, D–F). Of interest, IHC staining showed an evident decrease of epithelial cell marker E-cadherin in atrophic tubules (Figure 9A) and an increase of α -SMA (Figure 9B) and FSP1 (Figure 9C) in the obstructed kidneys at day 15 after UO. Administration of NMDA managed to inhibit the reduction of E-cadherin and increase in α -SMA and FSP1, preserving the epithelial phenotype (Figure 9).

As measured by Sirius red staining, all kidneys at day 15 after UO showed a significant increase in interstitial collagen deposition compared with contralateral kidneys (Figure 8C), which was also evident after Masson-Trichrome staining (Figure 9D). NMDA-treated mice showed a significant decrease in interstitial collagen fibers in obstructed kidneys, as measured by Sirius red (Figure 8C) and confirmed by Masson-Trichrome (Figure 9D).

DISCUSSION

In this study, we described a new role for NMDAR in preserving renal tubular epithelial structure. Structural integrity of the renal epithelium is of vital importance in the maintenance of normal kidney function, and it depends in a great deal on the formation and preservation of intercellular contacts, where an important role is attributed to intracellular calcium.^{29,30} NMDAR is a heteromeric complex composed of highly orchestrated subunits, whose activation triggers a series of Ca^{2+} -mediated intracellular events.³¹ In our study, *in vitro* activation of

NMDAR is followed by an increase of intracellular Ca^{2+} , showing that NMDAR in HK-2 is fully functional and its activation induces a fast and transient increase in intracellular Ca^{2+} . The basal activation of NMDAR in tubular cells is indispensable in the maintenance of the normal tubular epithelial phenotype. On the one hand, knockdown of NMDAR1 expression in HK-2 cells using shRNA induced changes in epithelial phenotype, evident as a decrease of E-cadherin and increase of α -SMA, along with the changes in cell morphology toward mesenchymal phenotype. On the other hand, activation of the channel in normal cells led to a decrease in basal cell motility and F-actin content, two key steps in EMT that are modulated by Ca^{2+} levels.^{21–23} Taken together, these results point to an indispensable role of basal NMDAR activity in the preservation of the epithelial phenotype of PTECs.

Tightness of adherens junctions, and thus stability of the epithelial phenotype, relies on cadherin–catenin complexes linked to the actin cytoskeleton. These complexes are disrupted in EMT caused by TGF- β 1, a potent inducer of fibrosis.^{32,33} In our model, after addition of TGF- β 1, HK-2 started disassociating from neighboring cells and acquired spindle-shaped morphology, accompanied by the reorganization of the actin cytoskeleton and elevated cell migration. Furthermore, cells lost epithelial marker E-cadherin, showed translocation of β -catenin into the nucleus, and acquired myofibroblast markers such as α -SMA and vimentin. Treatment with NMDA blunted all changes induced by TGF- β 1, showing that the activation of the channel was able to preserve the epithelial phenotype in cells undergoing EMT.

Acquisition of migratory phenotype and reorganization of actin cytoskeleton are prerequisites for effective migration of transformed cells through the basement membrane toward the interstitium. Being aware of the existence of biochemical and functional interactions between NMDAR subunits and cytoskeletal proteins,^{34,35} we sought to examine the influence of NMDAR activation on migration and F-actin distribution in HK-2. We showed by two independent *in vitro* migration assays that the activation of NMDAR has an inhibitory effect on cell migration. Cell velocity data support the wound and transwell migration results and confirm the role of NMDAR in the regulation of human PTEC migration. In addition, activation of NMDAR decreases basal actin polymerization state and TGF- β 1-induced actin reorganization in HK-2. The effect of NMDAR activation and Ca^{2+} on cell migration^{19,20} and actin organization^{26,27} has previously been reported in different cell types. Nahm *et al.*²⁰ showed that Ca^{2+} entry through activated NMDAR inhibited keratinocyte outgrowth and migration. Kihara *et al.*¹⁹ reported that stimulation of NMDAR inhibited neuronal migration in embryonic rat cerebral cortex. Furthermore, Cristofanilli and Akopian²⁷ showed that the NMDAR activation and influx of Ca^{2+} caused a reduction of F-actin in retinal neurons of salamander, whereas NMDAR activation in rat cerebellar granule cells rapidly shifted F/G-actin equilibrium in favor of depolymerization.²⁶

The role of NMDAR in preservation of tubular epithelial

phenotype was further confirmed in *in vivo* studies, in a mouse model of tubulointerstitial fibrosis induced by UUO. Consistent with the *in vitro* results, significant changes in cell phenotype were seen in renal tubules in the obstructed kidneys such as downregulation of E-cadherin, increase in α -SMA expression and FSP1 immunostaining, and interstitial collagen deposition. We provide evidence that NMDA treatment may attenuate renal fibrosis induced by UUO by preserving the epithelial phenotype, as shown by the inhibition of the decrease in E-cadherin induced by UUO. Furthermore, in obstructed kidneys of NMDA-treated mice, markers of the mesenchymal phenotype (FSP1 and α -SMA) were reduced, together with collagen deposition, pointing to NMDAR as a possible therapeutic target to slow down the progression of renal fibrosis.

The mechanism behind the effect of NMDA on tubular EMT seems to be related to the regulation of the activation of Ras pathway. Ras is one of the most common pathways leading to the activation of Erk and Akt, which represent important signaling events responsible for TGF- β 1-induced EMT in different epithelial cell types.^{36–38} A growing body of evidence describes the role of TGF- β 1 in the activation of Ras pathway.^{39–41} In our own hands, TGF- β 1 treatment induced rapid activation of Ras in HK-2 cells, which was blunted by co-treatment with NMDA. This effect of NMDA inhibiting the Ras pathway has previously been reported. Chandler *et al.*⁴² described that different levels of Ca^{2+} influx through NMDAR could activate opposing stimulatory and inhibitory pathways that regulate Erk activation and suggested the presence of a Ca^{2+} -activated inhibitory pathway that can attenuate Ras/Erk signaling. Ivanov *et al.*⁴³ and Sutton and Chandler⁴⁴ showed that NMDAR-dependent activating/inactivating pathways are spatially separated in neurons and that extrasynaptic NMDARs, containing NR2B subunit, mediate Erk inactivation. Finally, Kim *et al.*⁴⁵ showed that NMDAR activation could have differential effects on Ras/Erk pathway in neurons depending of the receptor subunit composition, showing that the NR2B subunit is coupled to the inhibition rather than the activation of the Ras/Erk pathway.⁴⁵ Our results showed that, in HK-2, the NR2B subunit was the main NR2 subunit expressed. Downregulation of the Ras pathway by NMDA supports the subunit-regulatory hypothesis and suggests that Ca^{2+} influx through NR2B-NMDAR in HK-2 could be responsible for the inactivation of Ras and subsequently Erk and Akt pathways.

It is well known that Snail1 acts as a key regulator of EMT by suppressing E-cadherin transcription and modulating tight junction protein expression,^{46–48} and it is crucial in initiation and progression of EMT.^{46,49} Moreover, it has been shown that Smad3 is necessary for TGF- β 1-induced Snail1 gene expression in a study using Smad3-null mice.⁵⁰ Our results showed upregulation of Snail1 and translocation of pSmad2/3 into the nucleus after treatment with TGF- β 1, which was blunted by co-treatment with NMDA, providing more proof of the inhibitory effect of NMDA on EMT of PTECs. Additionally, pharmacologic blockade using an antagonist of NMDAR (MK-801) in cells treated with TGF- β 1 and NMDA eliminated downregulation of Snail1 induced by

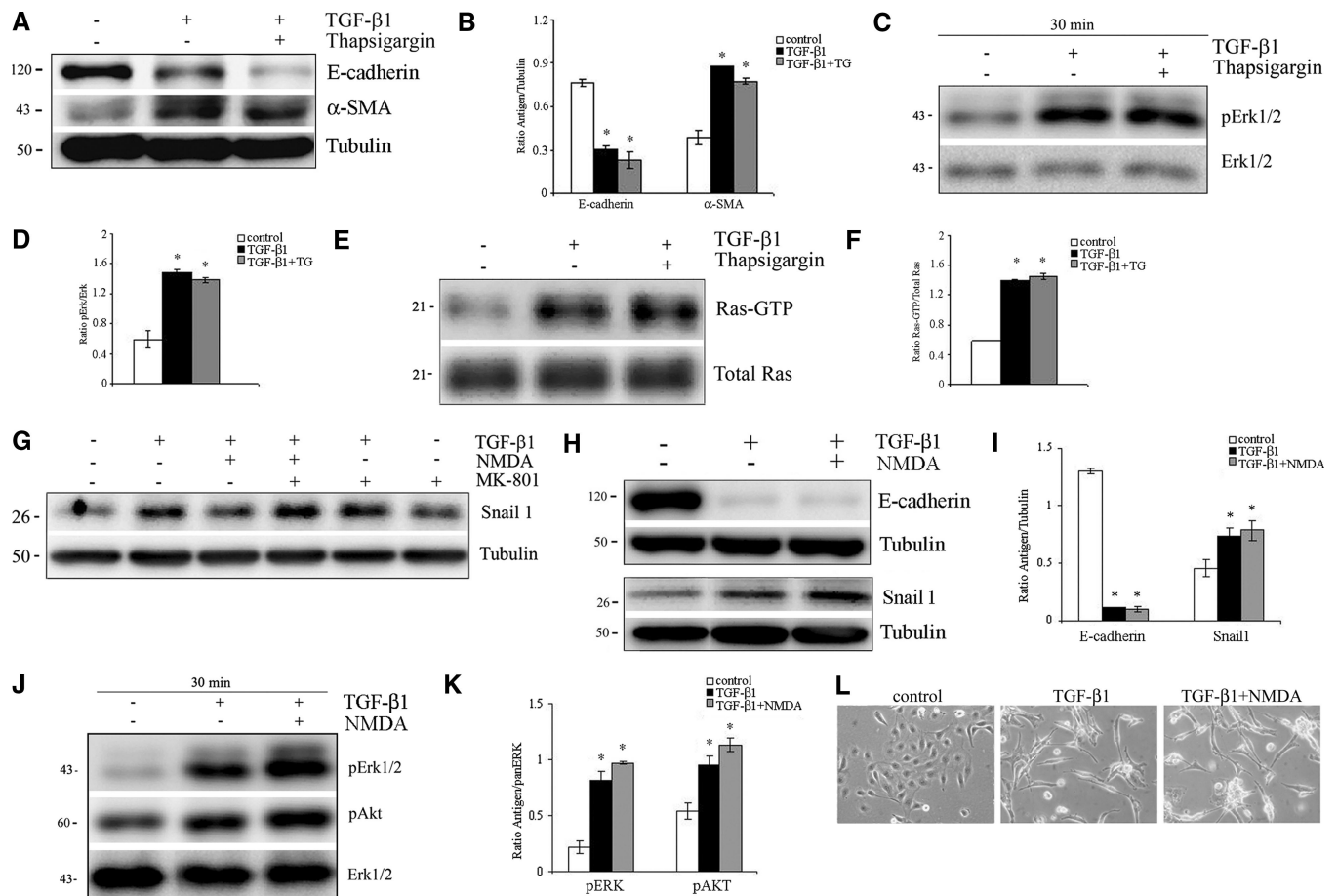


Figure 4. Calcium influx through NMDAR is responsible for the attenuation of TGF- β 1-induced tubular EMT. (A–F) Thapsigargin does not have the same inhibitory effect as NMDA treatment on TGF- β 1-induced alterations in HK-2 cells. HK-2 cells were incubated in serum-free media (control), TGF- β 1, or TGF- β 1 + Thapsigargin for 72 hours (E-cadherin and α -SMA), 30 minutes (pErk), and 10 minutes (Ras-GTP). Representative Western blots (A, C, and E) and quantitative analysis (B, D, and F) show that the incubation of HK-2 with TGF- β 1 and TG for indicated periods of time did not have the same effect as NMDA treatment on expression of E-cadherin and α -SMA (A and B) nor induced decreases in phosphorylation of Erk (C and D). (E) Total cell extracts were prepared and incubated with GST-RBD to measure the amount of Ras-GTP (top panel). Aliquots of total cell lysates (10 μ g) were run in parallel for detection of total Ras protein (bottom panel). Co-incubation of TG and TGF- β 1 did not induce deactivation of Ras, pointing to a specific effect of Ca²⁺ entry through NMDAR. (B, D, and F) * P < 0.05 versus control. (G) Co-incubation of cells with MK-801 abolished the inhibitory effect of NMDA on TGF- β 1-induced overexpression of Snail1. HK-2 cells were incubated for 6 hours in serum-free medium (control), TGF- β 1, TGF- β 1 + NMDA, TGF- β 1 + NMDA + MK-801, TGF- β 1 + MK-801, and MK-801 alone. Whole cell lysates were immunoblotted with antibody against Snail1. The samples were reprobbed with antibody against tubulin to ensure equal loading. (H–L) NMDAR activation failed to ameliorate TGF- β 1-induced alterations in HK-2 cells in the absence of Ca²⁺ in the culture media. HK-2 cells were incubated in serum free medium (control), TGF- β 1, or TGF- β 1 + NMDA (in serum free EpiLife [Ca²⁺-free] medium) for 72 hours (E-cadherin), 6 hours (Snail), and 30 minutes (pErk, pAkt). Representative Western blots (H and J) and quantitative analysis (I and K) show decreases in E-cadherin, increases in Snail 1 expression, and phosphorylation of Erk and Akt induced by TGF- β 1. Co-treatment with NMDA in Ca²⁺-free medium does not modify TGF- β 1 effects. (I and K) * P < 0.05 versus control. (L) Light microscopy shows morphologic changes caused by TGF- β 1 and NMDA treatment in Ca²⁺-free medium. Magnification: \times 20.

NMDA, showing that the above described effects are NMDAR specific. These results could also be explained by the inhibition of Ras activation with NMDA. It has been shown that the inhibition of Erk phosphorylation decreases TGF- β 1-induced Smad phosphorylation.^{51,52} Furthermore, it has also been shown that Ras activation is necessary to increase Snail expression induced by TGF- β 1.⁵³ Thus, a decrease in Ras activation could explain both the decrease in the activation of the Erk pathway and the Smad pathway.

To show that the described changes are the consequence of Ca²⁺ influx exclusively through NMDAR, we used TG, which has been previously shown to raise intracellular Ca²⁺ concentrations in proximal tubular cells in culture.⁵⁴ Treatment with TG did not lead to the recovery of E-cadherin and α -SMA expression modified by TGF- β 1. Additionally, simultaneous incubation of HK-2 with TGF- β 1 and TG did not prevent the activation of Ras and induced strong phos-

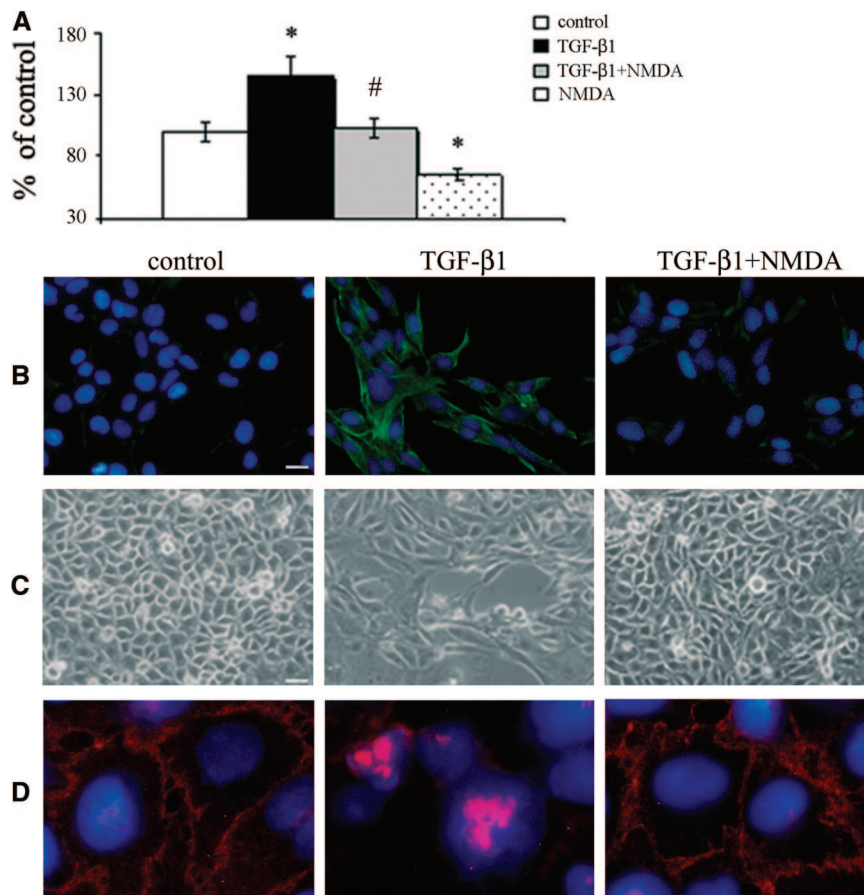


Figure 5. NMDAR activation modulates important key steps in tubular EMT *in vitro*. (A) Activation of NMDAR decreases basal actin polymerization state and TGF-β1–induced actin reorganization in HK-2 cells. Cells were grown in control conditions, TGF-β1, TGF-β1 + NMDA, and NMDA for 24 hours and examined by flow cytometry using Phalloidin fluorescence detected on FL1 (as described in Concise Methods). Values are given as percentage of the control (means ± SEM) of three independent experiments assayed in triplicate for every condition. * $P < 0.05$ versus control; # $P < 0.05$ versus TGF-β1. Immunofluorescence staining for the distribution of vimentin (B) and β-catenin (D) in HK-2 cells after incubation with TGF-β1 or TGF-β1 + NMDA. TGF-β1 induced *de novo* expression of vimentin (72 hours) and translocation of β-catenin (24 hours) into the nucleus. Co-treatment with NMDA reduced vimentin expression and restored β-catenin to the cell periphery. (C) Light microscopy shows morphologic changes caused by TGF-β1 and NMDA treatment. Scale bar (B) 10 μm; (C) 20 μm. (D) Original magnification: ×40.

phorylation of Erk1/2, showing that Ca^{2+} derived from other sources did not have the same effect on preservation of epithelial phenotype as Ca^{2+} influx through NMDAR. Furthermore, in the absence of Ca^{2+} in the medium, NMDA treatment failed to ameliorate TGF-β1–induced changes in expression of E-cadherin and Snail, as well as in phosphorylation of Erk1/2 and Akt. These results point to a specific role of Ca^{2+} entry through the activated NMDAR in maintaining the epithelial phenotype of PTECs.

Ca^{2+} entry via NMDAR activates type I NO synthase, which subsequently leads to vasodilatation in brain.⁵⁵ The kidney also contains type I NO synthase and vasodilates as a result of NMDAR activation.¹⁶ Thus, there is a possibility that NMDA

administration could ameliorate renal fibrosis *in vivo* by a combined effect of inhibition of tubular EMT and vasodilatation. Further studies in this direction are required to explore this possibility.

In conclusion, basal NMDAR activation is essential for the maintenance of the epithelial phenotype of PTECs. Furthermore, activation of tubular NMDAR attenuates EMT by blunting the TGF-β1–induced activation of Ras and the following cascades. Although no therapies aimed to increase NMDAR activation are available clinically, results obtained in this study identified a new therapeutic target for the inhibition of EMT and treatment of related diseases.

CONCISE METHODS

In Vitro Study

Cell Culture and Treatments.

HK-2 cells⁵⁶ obtained from ATCC were maintained in DMEM/F12 media (Life Technologies) supplemented with 2% FBS, HEPES buffer, insulin, transferrin, sodium selenite, glucose, dexamethasone, EGF, penicillin, and streptomycin (Sigma Aldrich). Fresh growth medium was changed every 2 to 3 days. Before treatments, cells were growth arrested in serum-free medium and incubated separately with serum-free medium (control), TGF-β1 (1.3 ng/ml; R&D Systems, Minneapolis, MN), TGF-β1 + NMDA (0.5 mM; Sigma Aldrich), TGF-β1 + TG (2 μM), TGF-β1 + MK-801 (NMDAR antagonist; 0.1 mM), MK-801, or NMDA alone for indicated periods of time. Cells were maintained according to the described protocol, unless otherwise indicated. For the experiments in Ca^{2+} -free conditions, EpiLife (calcium free) medium was purchased from Life Technologies.

Digital Video Imaging of Ca^{2+} Influx.

Cells were grown on glass coverslips in 2% FBS/DMEM/F12. After reaching an adequate confluence, cells were washed with KREBS solution (145 mM NaCl, 5 mM KCl, 2 mM CaCl_2 , 1 mM MgCl_2 , 10 mM HEPES buffer, and 11 mM glucose at pH 7.5) and incubated with 5 μM of Fluo-4AM (Molecular Probes) for 30 minutes at 37°C. Coverslips were assembled in a specific adaptor for the confocal microscope (Nikon TE-200), and digital video imaging of Ca^{2+} influx was done over a 20-minute interval after treatment with NMDA (0.5 mM). Images were taken every minute using ×100 objective at 485 nm of excitation and 528 nm of emission. For the control of the maxi-

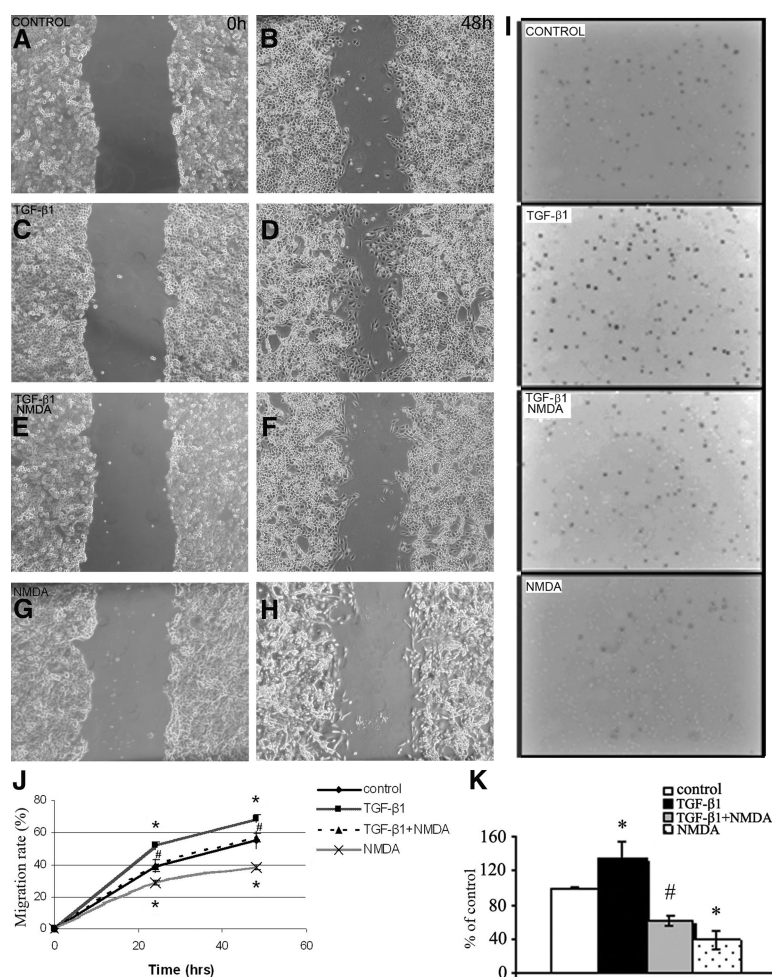


Figure 6. NMDAR activation inhibits basal and TGF- β 1-stimulated PTEC migration in vitro. (A–H) Wound healing assay. Contrast phase micrographs of HK-2 cells migrating into the denuded area of the scratch wound at various times after monolayer wounding. One representative experiment is shown to illustrate the wound closure after 48 hours in control conditions (B), TGF- β 1 (D), TGF- β 1 + NMDA (F), and NMDA (H) compared with the corresponding wounds at the point 0 hours for the control (A), TGF- β 1 (C), TGF- β 1 + NMDA (E), and NMDA (G). (A–H) Magnification: $\times 4$. (I) Transwell migration assay. Representative photos show parts of transwell inserts for control, TGF- β 1, TGF- β 1 + NMDA, and NMDA treated group of cells after 24 hours of incubation. Nuclei were stained with Hoechst. Magnification: $\times 20$. Quantification of cell migration in wound healing assay after 24 and 48 hours (J) and transwell migration assay after 24 hours (K). Data are presented as means \pm SEM (wound-healing assay) or percentage of control (means values \pm SEM; transwell migration assay) of three independent experiments assayed in triplicate for each time point and condition. (J) $*P < 0.05$ versus control at both time points and $\#P < 0.05$ versus TGF- β 1 at both time points. (K) $*P < 0.05$ versus control; $\#P < 0.05$ versus TGF- β 1.

imum level of fluorescence we used 10 μ M ionomycin (a calcium ionophore), and for the control of the minimum level of fluorescence, 5 mM EGTA was used.

Flow Cytometry Analysis of Filamentous Actin (F-Actin).

To investigate the possible effect of TGF β -1 and NMDA on filamentous actin in HK-2 cells, flow cytometry analysis was used. After 24

hours of incubation in described treatments, cells were washed in PBS and briefly exposed to Trypsin-EDTA (0.05%). Trypsinization was stopped by dilution with 2% FBS/DMEM/F12, and suspended cells were centrifuged at 2000 rpm for 5 minutes. Cell pellets were washed in PBS and centrifuged at 2000 rpm for 5 minutes. HK-2 were fixed in 4% paraformaldehyde/PBS for 10 minutes, washed in PBS, and incubated with 0.1% Triton X-100/PBS for 5 minutes. After centrifugation at 2000 rpm for 5 minutes, cells were incubated with 1% BSA/PBS for 30 minutes. Cells were stained with Alexa Fluor 488 phalloidin (Molecular Probes; dilution 1/150 in 1% BSA/PBS) for 1 hour in the dark. Ten thousand HK-2 cells were aspirated into a flow cytometer (Epics XL flow cytometer). The resulting histogram is a measure of phalloidin staining per cell, which is indicative of the amount of F-actin structure to which the fluorescence phalloidin is bound.

In Vitro Wound Migration Assay.

HK-2 cells were grown until 100% of confluence and were growth-arrested in serum-free medium for 24 hours. Cell monolayer was injured in a linear fashion with a sterile 200- μ l pipette tip and gently washed with PBS. Treatments were added, and the closure of the denuded area was monitored using a LEICA Microsystems DFC480 inverted microscope. Digital images were obtained at 0, 24, and 48 hours (four images per treatment). The width of the wounds was measured using LEICA Quantity Software IM50 Image Manager V.4.0, and the progression of migration was computed by subtracting the width of the wound at 24 or 48 hours from the initial width of the wound (at 0 hours). The experiments were repeated three times, and every treatment group was done in triplicate.

Transwell Migration Assay.

Transwell inserts (8- μ m porosity; Falcon, BD Labware) were coated with 20 μ l of growth factor-free Matrigel (BD Bioscience) and incubated at 37°C for 30 minutes. After serum deprivation, HK-2 cells were seeded (5×10^4) in the top well chambers in 200 μ l of DMEM/F12 with 0% FBS. The bottom compartments of transwell chambers were filled with 500 μ l of DMEM/F12 with 10% FBS. Media in the top and bottom chambers were supplemented with the same concentrations of corresponding treatments. After 24 hours, media were removed; cells were washed with PBS and fixed with 4% paraformaldehyde for 10 minutes and 0.1% Triton X-100 for 5 minutes. Cells that remained on the upper

variation, HK-2 cells were seeded (5×10^4) in the top well chambers in 200 μ l of DMEM/F12 with 0% FBS. The bottom compartments of transwell chambers were filled with 500 μ l of DMEM/F12 with 10% FBS. Media in the top and bottom chambers were supplemented with the same concentrations of corresponding treatments. After 24 hours, media were removed; cells were washed with PBS and fixed with 4% paraformaldehyde for 10 minutes and 0.1% Triton X-100 for 5 minutes. Cells that remained on the upper

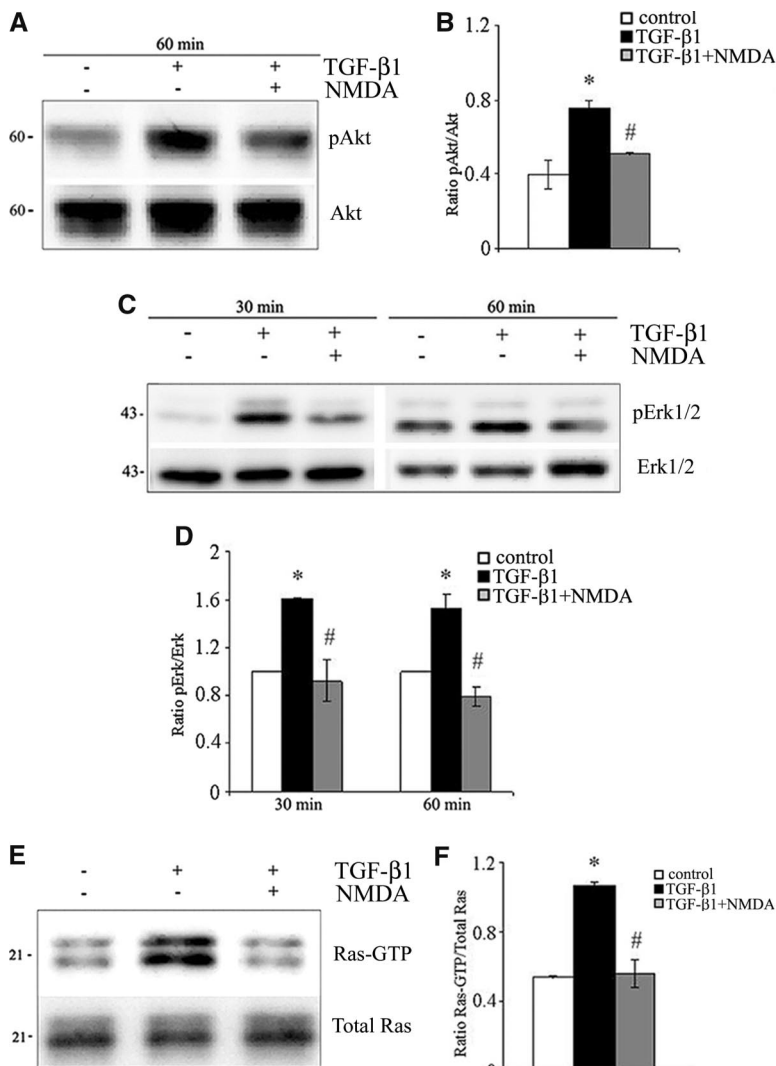


Figure 7. NMDAR activation reduced phosphorylation of Erk and Akt and activation of Ras induced by TGF- β 1 treatment. HK-2 cells were incubated in serum-free medium (control), TGF- β 1, or TGF- β 1 + NMDA for 30 and 60 (pErk, pAkt) and 10 minutes (Ras-GTP). Representative Western blots (A, C, and E) and quantitative analysis (B, D, and F) show alterations in protein expression induced by TGF- β 1 in HK-2 cells. NMDA treatment reduced phosphorylation of Akt (A and B) and Erk (C and D) induced by TGF- β 1 in HK-2 cells. After incubation with different treatments, whole cell lysates were immunoblotted with either phospho-Akt or total-Akt and phospho-Erk or total-Erk. (E and F) NMDA reduced TGF- β 1-induced activation of Ras. Total cell extracts were prepared and incubated with GST-RBD to measure the amount of Ras-GTP (top panel). Aliquots of total cell lysates (10 μ g) were run in parallel for detection of total Ras protein (bottom panel). (B, D, and F) * P < 0.05 versus control, # P < 0.05 versus TGF- β 1.

side of the filter membranes were gently removed with a cotton swab. Membranes were cut out from the inserts with a scalpel blade, and the cells from the bottom side of the membrane were stained with 1% Hoechst (Sigma) (cell nuclei) for 10 minutes at room temperature. Membranes were mounted on microscope slides using ProLong antifade reagent (Molecular Probes), with the lower surface facing up. Cells/nuclei were counted and analyzed using a LEICA Microsystems DFC480 fluorescence microscope. Fifty random fields were examined, and the results were plotted as

the percentage of control. The experiments were repeated three times, and every treatment group was performed in triplicate.

Live Cell Microscopy.

See Supplementary Material.

Analysis of Cell Migration in Time-Lapse Movies.

See Supplementary Material.

Protein Nuclear Extraction.

HK-2 cells were serum deprived for 24 hours and subsequently incubated in serum-free medium (control), TGF- β 1, and TGF- β 1 + NMDA for 120 minutes. After incubation, cells were washed with cold PBS. Nuclear protein fraction was extracted using the NE-PER Nuclear and Cytoplasmic Extraction KIT (Pierce).

Expression of Fusion Protein GST-RBD Raf1 in Escherichia coli.

See Supplementary Material.

Determination of Ras Activation.

Ras activation was assessed by specific binding of Ras-GTP (activated form) to the Ras binding domain of Raf-1. For determination of Ras-GTP, HK-2 cells were treated separately with serum-free medium (control), TGF- β 1, TGF- β 1 + NMDA, and TGF- β 1 + TG. After treatments, cells were incubated with magnesium containing lysis buffer (25 mM HEPES [pH 7.5], 150 mM NaCl, 1% NP-40, 0.25% Na-deoxycholate, 10% glycerol, 25 mM NaF, 10 mM MgCl₂, 1 mM EDTA, 1 mM Na₃VO₄, 2 mM PMSF, and protease inhibitor cocktail) for 10 minutes at 4°C. Cells were cold centrifuged for 10 minutes at 10,000 rpm, and supernatant was collected. After measurement of protein concentrations, 10 μ g of lysate proteins was used in the detection of total Ras after mixing with Laemmli sample buffer and boiling for 5 minutes. Seventy micrograms of lysate proteins was incubated with 2 μ g of GST-RBD precoupled with glutathione-Sepharose at 4°C for 2 hours. The sepharose conjugates were recovered by short centrifugation, washed two times with magnesium containing lysis buffer, resuspended in Laemmli sample buffer, and boiled for 5 minutes. Sample supernatants were subjected to 15% SDS-PAGE and used in Western blot detection of Ras-GTP.

Lentiviral Production and Infection of HK-2.

The shRNA vector was constructed by annealing complementary 60-mer oligonucleotides containing the 21-nucleotide target se-

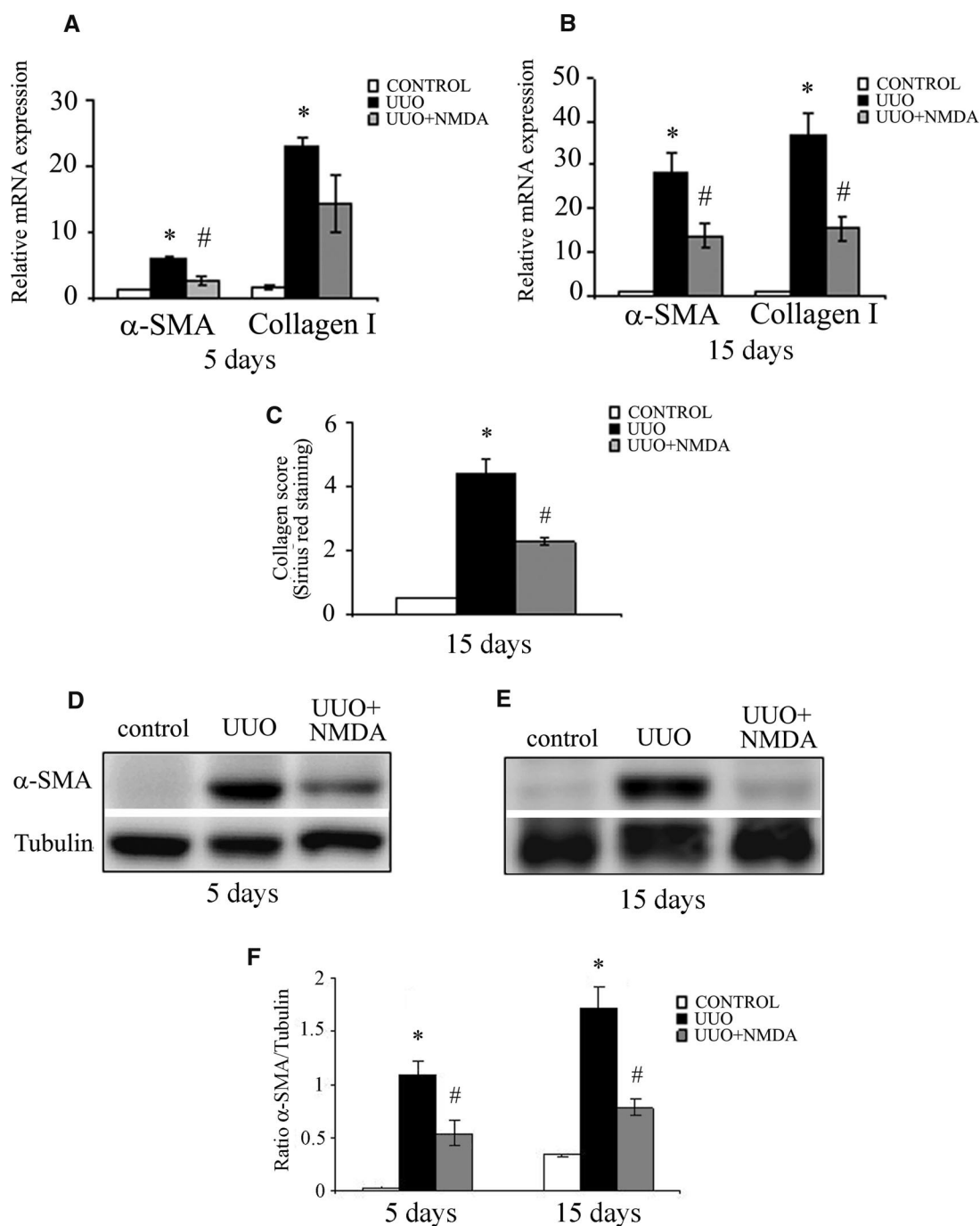


Figure 8. NMDA treatment reduced α -SMA and collagen I expression in the obstructed mouse kidney. (A and B) Real-time PCR analysis shows downregulation of α -SMA and collagen I mRNA expression in obstructed mouse kidney after NMDA treatment in different time points (5 and 15 days). Relative mRNA levels were calculated and expressed as fold induction over contralateral controls (value = 1.0) after normalizing with GAPDH. * $P < 0.05$ versus control; # $P < 0.05$ versus UUO. (C) Quantification of collagen content after Sirius red staining. Data are means \pm SEM of seven animals per group ($n = 7$). * $P < 0.05$ versus control; # $P < 0.05$ versus UUO. (D and E) Western blot shows increased expression of α -SMA in the obstructed kidneys at 5 and 15 days after UUO and inhibition of α -SMA in the UUO + NMDA group of mice. Whole kidney lysates were processed for protein analysis at days 5 (D and F) and 15 (E and F) after UUO and were immunoblotted with antibodies against α -SMA and tubulin, respectively. (F) * $P < 0.05$ versus control; # $P < 0.05$ versus UUO.

quence in both the sense and antisense orientation separated by a 9-nt spacer. The 21-mer sequence to NMDAR1 was CGCCAAC-TACAGCATCATGAA and is predicted to be specific only for

NMDAR1 as determined by BLAST database searches. Oligonucleotides to produce shRNA were annealed in buffer (150 mM NaCl; 50 mM Tris, pH 7.6) and cloned into the AgeI-BamHI site of

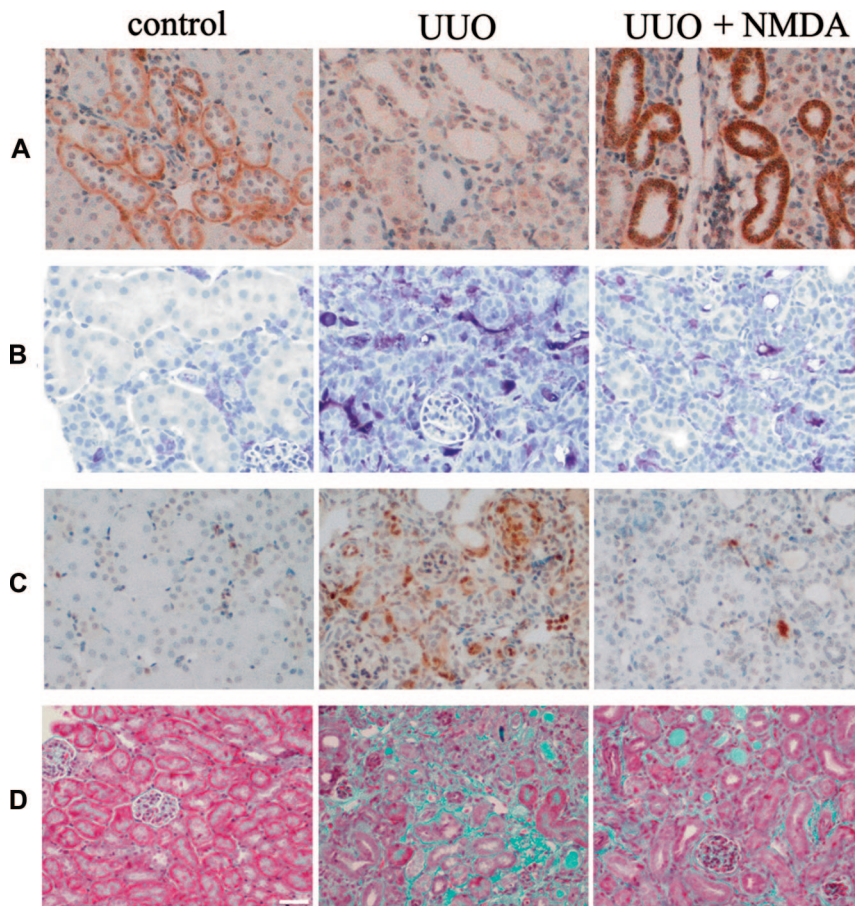


Figure 9. Activation of NMDAR in the mouse kidney attenuates renal fibrosis induced by UUO; immunohistochemical staining for E-cadherin, α -SMA, FSP1, and collagen I. Administration of NMDA reduced the loss of E-cadherin (A) and decreased α -SMA (B), FSP1 (C), and collagen I (D) expression in the obstructed mouse kidney 15 days after UUO. Kidney sections were stained with antibodies against E-cadherin (A), α -SMA (B), FSP1 (C), and with Masson-Trichrome staining (D). Representative photomicrographs of kidney sections from three investigated groups of mice are presented. (A–C) Original magnification: $\times 20$. (D) Scale bar, 20 μ m.

lentiviral vector for RNA interference-mediated gene silencing under the control of U6 promoter for expression of short hairpin shRNAs and the Venus variant of GFP under the control of SV40 promoter for monitoring transduction efficiency. To produce infective lentiviral particles, 293T cells were co-transfected by the polyethylenimine method with the virion packaging elements (VSV-G and $\Delta 8.9$) and the shRNA-producing vector (FSVsi-NMDAR1 or FSVsi as a control). 293T cells were allowed to produce lentiviral particles for 3 days in DMEM (Life Technologies) supplemented with 10% FBS, sodium pyruvate, nonessential amino acid, penicillin, and streptomycin. Culture medium was collected and centrifuged at 3000 rpm for 10 minutes; supernatant was collected and filtered using Sartorius filters at 4000 rpm for 30 minutes. Filtered supernatant was added to the growing culture of HK-2 cells and incubated overnight. Next day, fresh medium was replaced, and the cells were grown for an additional 3 to 4 days to allow endogenous gene knockdown. Western blot and real-time PCR were performed to check for gene knockdown.

In Vivo Study

This study was performed on female mice (B6CJ) weighing 18 to 22 g, obtained from Charles River (Barcelona, Spain). Mice were housed and maintained in a barrier facility, and pathogen-free procedures were used in all mouse rooms. Animals were kept in a 12-hour light/dark cycle at 22°C with *ad libitum* access to food and water. Mice were randomly assigned to two groups with seven mice each. Under general anesthesia, mice were subjected to UUO by double-ligating the left ureter using 2-0 silk after a lateral abdominal incision. The UUO + NMDA mice received NMDA treatment 3 days before and every day after the surgery (20 mg/kg body weight, intraperitoneally). UUO mice received injections of the same volume of the vehicle (0.9% saline solution). Five and 15 days after the surgery, animals from each group were killed under general anesthesia. One part of the obstructed kidney was fixed in 4% paraformaldehyde/PBS for histologic examinations after embedding in paraffin. Another part was frozen and kept at -80°C for protein and mRNA extractions. All procedures performed in this study followed the National Institute of Health Guide for the Care and Use of Laboratory Animals.

Semiquantitative PCR and Real-Time PCR. See Supplementary Material.

Western Blot Analysis. See Supplementary Material.

Immunofluorescence Microscopy. See Supplementary Material.

Morphometric Analysis of Interstitial Fibrosis and IHC. See Supplementary Material.

Statistical Analysis

Statistical significance was evaluated by *t* test or by one-way ANOVA followed by a Tukey *post hoc* test (SPSS, Chicago, IL), as appropriate. Values of $P < 0.05$ were considered statistically significant. All data examined are expressed as mean \pm SEM.

ACKNOWLEDGMENTS

This work was supported by Grants FIS, PI07/0427, and REDINREN (16/06). M.B. is supported by the studentship of the Catalan Government. We thank A. Martinez, M. Freixenet, and P. Valcheva (IRB Lleida) for help and cooperation in the laboratory.

DISCLOSURES

None.

REFERENCES

- Thiery JP: Epithelial-mesenchymal transitions in tumour progression. *Nat Rev Cancer* 2: 442–454, 2002
- Kalluri R, Neilson EG: Epithelial-mesenchymal transition and its implications for fibrosis. *J Clin Invest* 112: 1776–1784, 2003
- Zeisberg M, Kalluri R: The role of epithelial-to-mesenchymal transition in renal fibrosis. *J Mol Med* 82: 175–181, 2004
- Stahl PJ, Felsen D: Transforming growth factor-beta, basement membrane, and epithelial-mesenchymal transdifferentiation: Implications for fibrosis in kidney disease. *Am J Pathol* 159: 1187–1192, 2001
- Iwano M, Plieth D, Danoff TM, Xue C, Okada H, Neilson EG: Evidence that fibroblasts derive from epithelium during tissue fibrosis. *J Clin Invest* 110: 341–350, 2002
- Rastaldi MP, Ferrario F, Giardino L, Dell'Antonio G, Grillo C, Grillo P, Strutz F, Muller GA, Colasanti G, D'Amico G: Epithelial-mesenchymal transition of tubular epithelial cells in human renal biopsies. *Kidney Int* 62: 137–146, 2002
- Yang J, Liu Y: Dissection of key events in tubular epithelial to myofibroblast transition and its implications in renal interstitial fibrosis. *Am J Pathol* 159: 1465–1475, 2001
- Haddad JJ: N-methyl-D-aspartate (NMDA) and the regulation of mitogen-activated protein kinase (MAPK) signaling pathways: A revolving neurochemical axis for therapeutic intervention? *Prog Neurobiol* 77: 252–282, 2005
- Monyer H, Sprengel R, Schoepfer R, Herb A, Higuchi M, Lomeli H, Burnashev N, Sakmann B, Seeburg PH: Heteromeric NMDA receptors: Molecular and functional distinction of subtypes. *Science* 256: 1217–1221, 1992
- Morhenn VB, Waleh NS, Mansbridge JN, Unson D, Zolotarev A, Cline P, Toll L: Evidence for an NMDA receptor subunit in human keratinocytes and rat cardiocytes. *Eur J Pharmacol* 268: 409–414, 1994
- Miglio G, Dianzani C, Fallarini S, Fantozzi R, Lombardi G: Stimulation of N-methyl-D-aspartate receptors modulates Jurkat T cell growth and adhesion to fibronectin. *Biochem Biophys Res Commun* 361: 404–409, 2007
- Patton AJ, Genever PG, Birch MA, Suva LJ, Skerry TM: Expression of an N-methyl-D-aspartate-type receptor by human and rat osteoblasts and osteoclasts suggests a novel glutamate signaling pathway in bone. *Bone* 22: 645–649, 1998
- Mentaverri R, Kamel S, Wattel A, Prouillet C, Sevenet N, Petit JP, Tordjmann T, Brazier M: Regulation of bone resorption and osteoclast survival by nitric oxide: Possible involvement of NMDA-receptor. *J Cell Biochem* 88: 1145–1156, 2003
- Leung JC, Travis BR, Verlander JW, Sandhu SK, Yang SG, Zea AH, Weiner ID, Silverstein DM: Expression and developmental regulation of the NMDA receptor subunits in the kidney and cardiovascular system. *Am J Physiol Regul Integr Comp Physiol* 283: R964–R971, 2002
- Parisi E, Almaden Y, Ibarz M, Panizo S, Cardus A, Rodriguez M, Fernandez E, Valdivielso JM: N-methyl-D-aspartate receptors are expressed in rat parathyroid gland and regulate PTH secretion. *Am J Physiol Renal Physiol* 296: F1291–F1296, 2009
- Deng A, Valdivielso JM, Munger KA, Blantz RC, Thomson SC: Vasodilatory N-methyl-D-aspartate receptors are constitutively expressed in rat kidney. *J Am Soc Nephrol* 13: 1381–1384, 2002
- Deng A, Thomson SC: Renal NMDA receptors independently stimulate proximal reabsorption and glomerular filtration. *Am J Physiol Renal Physiol* 296: F976–F982, 2009
- Giardino L, Armelloni S, Corbelli A, Mattinzoli D, Zennaro C, Guerrot D, Tourrel F, Ikehata M, Li M, Berra S, Carraro M, Messa P, Rastaldi MP: Podocyte glutamatergic signaling contributes to the function of the glomerular filtration barrier. *J Am Soc Nephrol* 20: 1929–1940, 2009
- Kihara M, Yoshioka H, Hirai K, Hasegawa K, Kizaki Z, Sawada T: Stimulation of N-methyl-D-aspartate (NMDA) receptors inhibits neuronal migration in embryonic cerebral cortex: a tissue culture study. *Brain Res Dev Brain Res* 138: 195–198, 2002
- Nahm WK, Philpot BD, Adams MM, Badiavas EV, Zhou LH, Butmarc J, Bear MF, Falanga V: Significance of N-methyl-D-aspartate (NMDA) receptor-mediated signaling in human keratinocytes. *J Cell Physiol* 200: 309–317, 2004
- Chaudhuri P, Colles SM, Damron DS, Graham LM: Lysophosphatidylcholine inhibits endothelial cell migration by increasing intracellular calcium and activating calpain. *Arterioscler Thromb Vasc Biol* 23: 218–223, 2003
- Schwab A: Function and spatial distribution of ion channels and transporters in cell migration. *Am J Physiol Renal Physiol* 280: F739–F747, 2001
- Janmey PA: Phosphoinositides and calcium as regulators of cellular actin assembly and disassembly. *Annu Rev Physiol* 56: 169–191, 1994
- Schwab A, Schuricht B, Seeger P, Reinhardt J, Dartsch PC: Migration of transformed renal epithelial cells is regulated by K⁺ channel modulation of actin cytoskeleton and cell volume. *Pflügers Arch* 438: 330–337, 1999
- Chitaev NA, Troyanovsky SM: Adhesive but not lateral E-cadherin complexes require calcium and catenins for their formation. *J Cell Biol* 142: 837–846, 1998
- Shorte SL: N-methyl-D-aspartate evokes rapid net depolymerization of filamentous actin in cultured rat cerebellar granule cells. *J Neurophysiol* 78: 1135–1143, 1997
- Cristofanilli M, Akopian A: Calcium channel and glutamate receptor activities regulate actin organization in salamander retinal neurons. *J Physiol* 575: 543–554, 2006
- White DP, Caswell PT, Norman JC: alpha v beta3 and alpha5beta1 integrin recycling pathways dictate downstream Rho kinase signaling to regulate persistent cell migration. *J Cell Biol* 177: 515–525, 2007
- Nigam SK, Rodriguez-Boulant E, Silver RB: Changes in intracellular calcium during the development of epithelial polarity and junctions. *Proc Natl Acad Sci USA* 89: 6162–6166, 1992
- Stuart RO, Nigam SK: Regulated assembly of tight junctions by protein kinase C. *Proc Natl Acad Sci USA* 92: 6072–6076, 1995
- Ghosh A: Neurobiology. Learning more about NMDA receptor regulation. *Science* 295: 449–451, 2002
- Tian YC, Phillips AO: Interaction between the transforming growth factor-beta type II receptor/Smad pathway and beta-catenin during transforming growth factor-beta1-mediated adherens junction disassembly. *Am J Pathol* 160: 1619–1628, 2002
- Masszi A, Fan L, Rosivall L, McCulloch CA, Rotstein OD, Mucci I, Kapus A: Integrity of cell-cell contacts is a critical regulator of TGF-beta 1-induced epithelial-to-myofibroblast transition: Role for beta-catenin. *Am J Pathol* 165: 1955–1967, 2004
- Lei S, Czerwinski E, Czerwinski W, Walsh MP, MacDonald JF: Regulation of NMDA receptor activity by F-actin and myosin light chain kinase. *J Neurosci* 21: 8464–8472, 2001
- Hardingham GE, Bading H: The Yin and Yang of NMDA receptor signalling. *Trends Neurosci* 26: 81–89, 2003
- Xie L, Law BK, Chytil AM, Brown KA, Aakre ME, Moses HL: Activation of the Erk pathway is required for TGF-beta1-induced EMT in vitro. *Neoplasia* 6: 603–610, 2004
- Bakin AV, Tomlinson AK, Bhowmick NA, Moses HL, Arteaga CL: Phosphatidylinositol 3-kinase function is required for transforming growth factor beta-mediated epithelial to mesenchymal transition and cell migration. *J Biol Chem* 275: 36803–36810, 2000
- Grille SJ, Bellacosa A, Upson J, Klein-Szanto AJ, van Roy F, Lee-Kwon W, Donowitz M, Tsichlis PN, Larue L: The protein kinase Akt induces epithelial mesenchymal transition and promotes enhanced motility

- and invasiveness of squamous cell carcinoma lines. *Cancer Res* 63: 2172–2178, 2003
39. Reimann T, Hempel U, Krautwald S, Axmann A, Scheibe R, Seidel D, Wenzel KW: Transforming growth factor-beta1 induces activation of Ras, Raf-1, MEK and MAPK in rat hepatic stellate cells. *FEBS Lett* 403: 57–60, 1997
 40. Yue J, Frey RS, Mulder KM: Cross-talk between the Smad1 and Ras/MEK signaling pathways for TGFbeta. *Oncogene* 18: 2033–2037, 1999
 41. Santibanez JF, Guerrero J, Quintanilla M, Fabra A, Martinez J: Transforming growth factor-beta1 modulates matrix metalloproteinase-9 production through the Ras/MAPK signaling pathway in transformed keratinocytes. *Biochem Biophys Res Commun* 296: 267–273, 2002
 42. Chandler LJ, Sutton G, Dorairaj NR, Norwood D: N-methyl D-aspartate receptor-mediated bidirectional control of extracellular signal-regulated kinase activity in cortical neuronal cultures. *J Biol Chem* 276: 2627–2636, 2001
 43. Ivanov A, Pellegrino C, Rama S, Dumalska I, Salyha Y, Ben Ari Y, Medina I: Opposing role of synaptic and extrasynaptic NMDA receptors in regulation of the extracellular signal-regulated kinases (ERK) activity in cultured rat hippocampal neurons. *J Physiol* 572: 789–798, 2006
 44. Sutton G, Chandler LJ: Activity-dependent NMDA receptor-mediated activation of protein kinase B/Akt in cortical neuronal cultures. *J Neurochem* 82: 1097–1105, 2002
 45. Kim MJ, Dunah AW, Wang YT, Sheng M: Differential roles of. *Neuron* 46: 745–760, 2005
 46. Lee JM, Dedhar S, Kalluri R, Thompson EW: The epithelial-mesenchymal transition: new insights in signaling, development, and disease. *J Cell Biol* 172: 973–981, 2006
 47. Barrallo-Gimeno A, Nieto MA: The Snail genes as inducers of cell movement and survival: implications in development and cancer. *Development* 132: 3151–3161, 2005
 48. Carrozzino F, Soulie P, Huber D, Mensi N, Orci L, Cano A, Feraille E, Montesano R: Inducible expression of Snail selectively increases paracellular ion permeability and differentially modulates tight junction proteins. *Am J Physiol Cell Physiol* 289: C1002–C1014, 2005
 49. Liu Y: Epithelial to mesenchymal transition in renal fibrogenesis: pathologic significance, molecular mechanism, and therapeutic intervention. *J Am Soc Nephrol* 15: 1–12, 2004
 50. Sato M, Muragaki Y, Saika S, Roberts AB, Ooshima A: Targeted disruption of TGF-beta1/Smad3 signaling protects against renal tubulointerstitial fibrosis induced by unilateral ureteral obstruction. *J Clin Invest* 112: 1486–1494, 2003
 51. Hayashida T, Decaestecker M, Schnaper HW: Cross-talk between ERK MAP kinase and Smad signaling pathways enhances TGF-beta-dependent responses in human mesangial cells. *FASEB J* 17: 1576–1578, 2003
 52. Rhyu DY, Yang Y, Ha H, Lee GT, Song JS, Uh ST, Lee HB: Role of reactive oxygen species in TGF-beta1-induced mitogen-activated protein kinase activation and epithelial-mesenchymal transition in renal tubular epithelial cells. *J Am Soc Nephrol* 16: 667–675, 2005
 53. Horiguchi K, Shirakihara T, Nakano A, Imamura T, Miyazono K, Saitoh M: Role of Ras signaling in the induction of snail by transforming growth factor-beta. *J Biol Chem* 284: 245–253, 2009
 54. Jan CR, Ho CM, Wu SN, Tseng CJ: Mechanism of rise and decay of thapsigargin-evoked calcium signals in MDCK cells. *Life Sci* 64: 259–267, 1999
 55. Faraci FM, Breese KR: Nitric oxide mediates vasodilatation in response to activation of N-methyl-D-aspartate receptors in brain. *Circ Res* 72: 476–480, 1993
 56. Ryan MJ, Johnson G, Kirk J, Fuerstenberg SM, Zager RA, Torok-Storb B: HK-2: an immortalized proximal tubule epithelial cell line from normal adult human kidney. *Kidney Int* 45: 48–57, 1994

Supplemental information for this article is available online at <http://www.jasn.org/>.